MOLECULAR AND CELLULAR BIOLOGY, Mar. 2002, p. 1488–1494 Vol. 22, No. 5
0270-7306/02/$04.00+0 DOI: 10.1128/MCB.22.5.1488–1494.2002

Embryonic Lethality Caused by Apoptosis during Gastrulation in Mice Lacking the Gene of the ADP-Ribosylation Factor-Related Protein 1

A. G. Mueller,[1] M. Moser,[2] R. Kluge,[3] S. Leder,[1] M. Blum,[4] R. Büttner,[2] H.-G. Joost,[1] and A. Schürmann[1]*

Institute of Pharmacology,[1] Institute of Pathology,[2] and Institute of Animal Research,[3] Medical Faculty, Technical University of Aachen, D-52057 Aachen, and Institute of Toxicology and Genetics, Forschungszentrum Karlsruhe, D-76021 Karlsruhe,[4] Germany

Received 4 October 2001/Returned for modification 27 November 2001/Accepted 6 December 2001

ADP-ribosylation factor (ARF)-related protein 1 (ARFRP1) is a membrane-associated GTPase with significant similarity to the family of ARFs. We have recently shown that ARFRP1 interacts with the Sec7 domain of the ARF-specific guanine nucleotide exchange factor Sec7-1/cytohesin and inhibits the ARF/Sec7-dependent activation of phospholipase D in a GTP-dependent manner. In order to further analyze the function of ARFRP1, we cloned the mouse *Arfrp1* gene and generated *Arfrp1* null-mutant mice by gene targeting in embryonic stem cells. Heterozygous *Arfrp1* mutants developed normally, whereas homozygosity for the mutant allele led to embryonic lethality. Cultured homozygous *Arfrp1* null-mutant blastocysts were indistinguishable from wild-type blastocysts. In vivo, they implanted and formed egg cylinder stage embryos that appeared normal until day 5. Between embryonic days 6 and 7, however, apoptotic cell death of epiblast cells occurred in the embryonic ectoderm during gastrulation, as was shown by histological analysis combined with terminal deoxynucleotidyltransferase-mediated dUTP-biotin nick end labeling. Epiblast cells that would normally differentiate to mesodermal cells detached from the ectodermal cell layer and were dispersed into the proamniotic cavity. In contrast, the development of extraembryonic structures appeared unaffected. Our results demonstrate that ARFRP1 is necessary for early embryonic development during gastrulation.

ADP-ribosylation factors (ARFs) are GTP-binding proteins that are involved in multiple steps of membrane trafficking and regulation of phospholipase D (PLD) (5, 15, 20, 24, 29). ARFRP1 (ARF-related protein 1), previously designated ARP (25), is a membrane-associated 25-kDa GTPase with remote similarity to ARF and ARF-like protein (33 and 39% identical amino acids to ARF1 and ARF-like 3, respectively). ARFRP1 contains all characteristic sequence motifs involved in nucleotide binding and GTP hydrolysis. Compared with other GTPases, guanine nucleotide exchange of recombinant ARFRP1 is slow but GTPase activity is high in the absence of an activating protein. In contrast to ARF and ARF-like proteins, ARFRP1 lacks the N-terminal myristoylation motif (glycine 2) necessary for membrane association. However, ARFRP1 is predominantly located in the plasma membrane and is absent from the cytosol (25), whereas ARF proteins shuttle between membranes and the cytosol, depending on the bound nucleotide (3). Previous studies have suggested that ARFRP1 is involved in a pathway inhibiting the ARF-controlled activity of PLD (26). ARFRP1 binds the ARF-specific nucleotide exchange factor Sec7-1/cytohesin in a GTP-dependent manner and inhibits the ARF/Sec7-dependent activation of PLD. In addition, transfection of HEK-293 cells with a constitutively active mutant of ARFRP1 inhibited the PLD stimulation induced by muscarinic acetylcholine receptor-3 and the translocation of ARF from the cytosol to membranes.

ARF and ARF-like proteins are highly conserved throughout the evolution of eukaryotes (29). In yeast, five members of the ARF-family have been identified (9, 14, 21, 22). The closest relative of ARFRP1 is yARF-like protein 3 (yARL3), with 43% identical amino acids (14). Disruption of the y*Arl3* gene resulted in enhanced cold sensitivity of growth and in retarded processing of alkaline phosphatase and carboxypeptidase Y at the nonpermissive temperature. Thus, it was suggested that yARL3 is involved in protein transport between endoplasmic reticulum, Golgi, and vacuole (14).

In order to characterize the function of ARFRP1 in a mammalian organism, we generated mice with a targeted disruption of the *Arfrp1* gene. It is shown here that homozygosity for the transgene causes embryonic lethality at gastrulation and apoptosis of ectodermal cells that would normally differentiate and form the mesodermal cell layer.

MATERIALS AND METHODS

Library screening and DNA sequencing. Genomic clones of *Arfrp1* were isolated by screening a 129 SvJ mouse genomic library (Lambda FIX II Vector; Stratagene, La Jolla, Calif.) with a cDNA probe derived from the rat ARFRP1 cDNA. Two clones were isolated and sequenced after fragmentation by sonication or digestion with restriction enzymes and subcloning into pUC18 and pGEM−5Zf(+). Sequencing was performed in both directions (Thermo-sequenase fluorescent-labeled primer cycle sequencing kit; Amersham Life Science, Little Chalfont, Bucks, United Kingdom) with the aid of an automated sequencer (LI-COR, Lincoln, Neb.).

Gene targeting. For generation of the targeting vector, a 5.6-kb clone in pGEM−5Zf(+) was used. The 595 bp containing exons 2 and 3, encoding the start codon, the PM1-PM3, and the G1 motifs, was replaced by a 1.1-kb neomycin resistance cassette introducing a diagnostic *Stu*I site. The targeting vector was linearized with *Not*I, and embryonic stem (ES) cells (129 SvJ) were transfected by electroporation. Cells were subsequently cultured in the presence of 400 μg of G418/ml for 12 days. A total of 288 neomycin-resistant ES clones were picked, and their genomic DNA was isolated and digested with *Stu*I. For the identification of homologous recombinants, Southern blots were performed with a 3′ external probe generated with a PCR fragment containing intron 4 (primers, 5′-GCAAAAGGAACCTGGAACTG-3′ and 5′-CTGAAAGTGCTCAACTCA

* Institute of Pharmacology, Medical Faculty, Technical University of Aachen, D-52057 Aachen, Germany. Phone: 49-241-8089137. Fax: 49-241-8082433. E-mail: aschuermann@ukaachen.de.

GG-3′). Two ES cell clones that had incorporated the targeting vector by homologous recombination were injected into C57Bl/6J blastocysts and subsequently were transferred into a pseudopregnant foster mouse. Male chimeric mice were mated with C57Bl/6J females. Genomic DNA was isolated from tail biopsies, digested with *Stu*I, and analyzed by Southern blotting with the 3′ external probe or by PCR with primers for amplification of both the *Arfrp1* and the *neo* gene (primer 1 [ARFRP1, 200 bp], 5′-GGTCCACAACCCAGCTGAC-3′; primer 2 [Neo, 440 bp], 5′-CGAGGATCTCGTCGTGCCC-3′; primer 3 [ARFRP1 reverse], 5′-CCCAAAACATGAGACGAGCCTTCC-3′).

Northern blot analysis. RNA was prepared from liver, kidney, and testis as described previously (4). Samples (15 μg) of total RNA were separated by electrophoresis on 1% (wt/vol) agarose gels containing 3% (vol/vol) formaldehyde and were transferred onto nylon membranes (Hybond N^+; Amersham-Pharmacia, Freiburg, Germany). Probes of the cDNA of rat ARFRP1 were generated with the Klenow fragment of DNA polymerase I and [α-^{32}P]dCTP by random oligonucleotide priming. The nylon membranes were hybridized at 42°C, and blots were washed twice with 0.8% SSC (1× SSC is 0.15 M NaCl plus 0.015 M sodium citrate) containing 0.1% sodium dodecyl sulfate.

Immunochemical detection of ARFRP1 in membranes from different tissues. Tissues (liver, kidney, and testis) were homogenized and centrifuged for 10 min at 600 × *g*. The supernatant was centrifuged at 200,000 × *g* at 4°C for 1 h. Resuspended membrane proteins (20 μg) were separated by sodium dodecyl sulfate–14% polyacrylamide gel electrophoresis and were transferred onto nitrocellulose. Immunochemical detection was performed with a polyclonal antiserum against recombinant ARFRP1 (25). Bound immunoglobulin was detected with ^{125}I-protein A.

In vitro culture of blastocysts. *Arfrp1*$^{+/-}$ mice were intercrossed in a 12-h mating period. At embryonic day 3.5 (E3.5), blastocysts were flushed from the uteri of plugged females and were cultured individually as described previously (12). After a resting period of 2 days, photographs were taken every 24 h. After 6 to 8 days in culture, the genotypes of the blastocysts were determined by PCR.

Histological analysis. Uteri from females plugged in a 12-h mating period were isolated at E5.5, 6.5, 7.5, and 8.5. Uteri were fixed in 4% paraformaldehyde, dehydrated, and embedded in paraffin. Serial sections (5 μm) were stained with hematoxylin and eosin.

Terminal deoxynucleotidyltransferase-mediated dUTP-biotin nick end labeling (TUNEL) assays. Apoptotic cells were detected in paraffin sections of mouse embryos of E5.5 to 8.5 with the aid of a TdT-FragEL DNA fragmentation detection kit (Oncogene Research Products, Boston, Mass.) according to the manufacturer's protocol. Sections were counterstained with methyl green.

RESULTS

Targeted disruption of the *Arfrp1* gene. Two genomic clones (13.5 kb and about 21 kb) comprising the total *Arfrp1* gene (accession number AJ413952) were isolated from a 129 SvJ library. The targeting construct was generated by exchange of exons 2 and 3, coding for the translation start and the essential nucleotide binding motifs PM1-PM3 and G1, for a neomycin resistance cassette. The construct (Fig. 1A) contained 3,015 bp of the 5′ flanking region and 1,963 bp of intron 4.

Transfection of ES cells with the targeting construct yielded four homologous recombinants in 288 transformants. Homologous recombination was ascertained by Southern blot analysis with an external probe (Fig. 1B). Injection of recombinant ES cells into blastocysts of C57BL/6 mice resulted in the generation of chimeric mice that were mated with C57BL/6 mice. F_1 mice carrying the transgene were interbred and yielded *Arfrp1*$^{+/+}$ and *Arfrp1*$^{+/-}$ mice with a frequency of 1:1.9 but yielded no *Arfrp1*$^{-/-}$ mutants out of 94 offspring (Fig. 1B). This result indicates that homozygous disruption of *Arfrp1* results in embryonic lethality.

ARFRP1 is expressed during embryonic development. In order to determine the ARFRP1 expression during embryonic development, a Northern blot analysis was performed with embryos of different stages. Figure 2 illustrates the time course of ARFRP1 expression between 4.5 and 18.5 days post-coitum (p.c.). ARFRP1 mRNA was already detected during early embryogenesis at day 4.5 p.c., increased during gastrulation and neurulation (E7.5 and 8.5), and remained high throughout embryogenesis, except for a decline at late stages of gestation (E17.5 and 18.5).

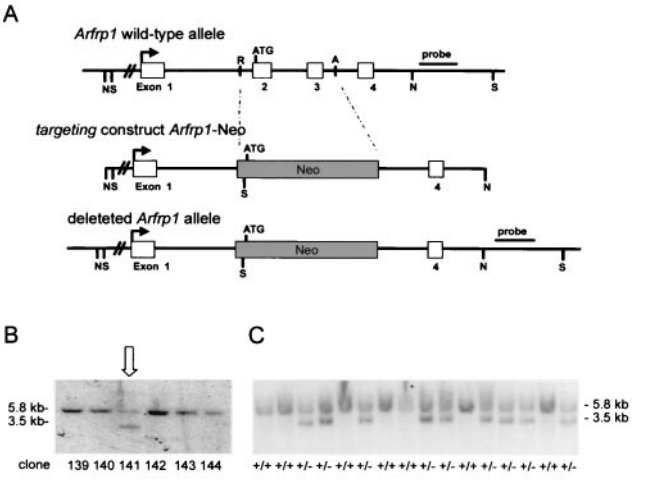

FIG. 1. Targeted disruption of the *Arfrp1* gene by homologous recombination. (A) Disruption strategy for *Arfrp1* showing the wild-type allele, the targeting construct, and the targeted *Arfrp1* allele. The *neo* cassette was inserted into the *Rsr*II and *Ava*II sites of exon 2 and intron 3, introducing a diagnostic *Stu*I site. Relevant restriction sites are shown (A, *Ava*II; N, *Nco*I; R, *Rsr*II; S, *Stu*I). The position of the 3′ probe for Southern blot analysis is indicated. (B) Southern blot of several ES cell clones; DNA was digested with *Stu*I and analyzed with the 3′ probe. The arrow depicts a clone that incorporated the targeting vector by homologous recombination; this clone was used for injection into blastocysts. (C) Southern blot analysis of *Stu*I-digested DNA from neonate tails after hybridization with a 3′ probe. The positions of the wild-type allele (5.8 kb) and the targeted allele (3.5 kb) are indicated.

Phenotype of heterozygous *Arfrp1* mutants. Mice heterozygous for the *Arfrp1* deletion were phenotypically normal and showed no difference in the development of body weight over

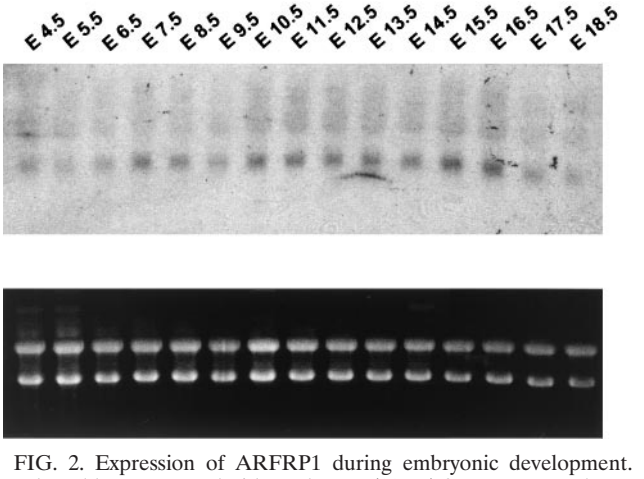

FIG. 2. Expression of ARFRP1 during embryonic development. Northern blots generated with total RNA (20 μg) from mouse embryos at different ages were purchased form Seegene (Seoul, Korea) and were hybridized as described in Materials and Methods with a cDNA of ARFRP1 (upper panel). Comparable amounts of RNA are present in each lane, as judged from ethidium bromide staining (lower panel).

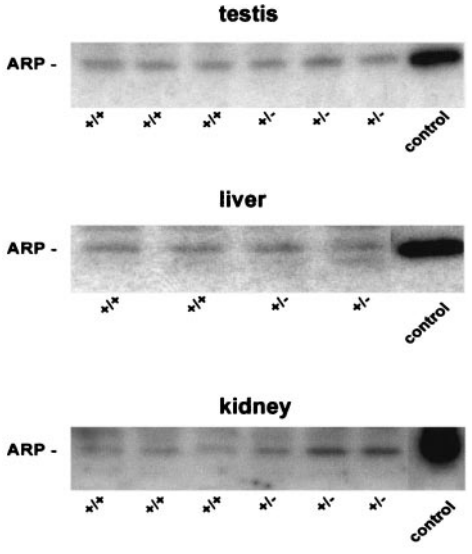

FIG. 3. Expression of ARFRP1 in tissues from *Arfrp1*$^{+/+}$ and *Arfrp1*$^{+/-}$ mice. Immunochemical detection of ARFRP1 in membranes of testis, liver, and kidney from *Arfrp1*$^{+/+}$ and *Arfrp1*$^{+/-}$ mice. Tissues of the indicated animals were homogenized, and 20 μg of the centrifuged (200,000 × *g*) pellet were analyzed in Western blots with an antiserum raised against recombinant ARFRP1.

a time course of 6 months (data not shown). There was no difference in ARFRP1 mRNA (data not shown) and protein levels in liver, kidney, and testis between wild-type mice and *Arfrp1*$^{+/-}$ mutants (Fig. 3), indicating that the deletion of one allele did not reduce expression of ARFRP1.

Characterization of *Arfrp1*$^{-/-}$ blastocysts. No viable *Arfrp1*$^{-/-}$ neonates were identified when heterozygous mice were intercrossed, indicating that homozygosity for the *Arfrp1* mutation causes embryonic lethality. To investigate the growth of *Arfrp1* mutant embryos, blastocysts (E3.5) from heterozygous matings were individually cultured in vitro, and outgrowth was monitored for 6 to 8 days. At the end of the experiment, genotypes of the blastocysts were determined by PCR (Fig. 4B). Among 32 cultured blastocysts obtained from 4 litters, *Arfrp1*$^{+/+}$, *Arfrp1*$^{+/-}$, and *Arfrp1*$^{-/-}$ blastocysts were identified at a ratio of 12:16:4. As is shown in Fig. 4A, the morphology of *Arfrp1*$^{-/-}$ blastocysts was indistinguishable from that of *Arfrp1*$^{+/+}$ and *Arfrp1*$^{+/-}$ blastocysts, with the trophoblast spreading out on the culture dish and a proliferating inner cell mass on top. This result indicates that *Arfrp1*$^{-/-}$ blastocysts were generated and that disruption of *Arfrp1* did not alter the growth of stem cells or the development of the blastocysts.

Deletion of *Arfrp1* results in embryonic lethality at the gastrulation stage (E6.5 to 7.5) and prevents differentiation of embryonic ectoderm. In order to determine the time point of death of *Arfrp1*$^{-/-}$ mutants, a histological analysis of uteri from heterozygous intercrosses was performed at different days of gestation. At E5.5 all embryos appeared normal (Table 1). At E6.5 to 8.5 about 25% of the embryos exhibited striking abnormalities (Table 1). In whole-mount preparations of embryos at E7.5, the egg cylinder of *Arfrp1*$^{-/-}$ mutants was markedly reduced in size, whereas the ectoplacental cone appeared unaffected (Fig. 5A). In contrast, wild-type and heterozygous embryos were indistinguishable (Fig. 5A and B).

Histological analysis of abnormal embryos revealed massive defects before and during gastrulation (Fig. 6). At E6.5, abnormal embryos could be recognized by profound alteration of the distal part of the egg cylinder. Rounded pyknotic cells were found within this area of the egg cylinder in the proamniotic cavity, and some of these were only loosely attached to the ectodermal cell layer (Fig. 6A and B, lower panels). In contrast, the proximal extraembryonic part of the embryo appeared normal. In order to determine whether the morphologically abnormal cells within the proamniotic cavity were apoptotic, TUNEL assays were performed with sections adjacent to those stained for histological examination. This analysis demonstrated that the pyknotic epiblast cells in the area of the primitive streak region were TUNEL positive and therefore were apoptotic. In contrast, normal egg cylinder stage embryos showed the typical organization with the outer epithelial layer, the visceral endoderm, and an inner epithelial sheet, the primitive ectoderm (Fig. 6A and B, upper panels). The proximal, extraembryonic endodermal cells are characterized by a columnar morphology with apical vacuoles, whereas the distal, embryonic endodermal cells have no vacuoles and show a squamous appearance. The ectoderm reveals marked differences between the embryonic and extraembryonic parts as well, with a much thicker epithelial organization of the distal embryonic cells (Fig. 6B, upper panel).

At E7.5, histological differences between control and mutant embryos were even more pronounced. Sagittal sections exhibited defects in the embryonic ectodermal cell layer and accumulation of dead cells within the amniotic cavity (Fig. 6C, lower panels). Transversal sections confirmed this observation and demonstrated that the abnormal embryo was disorganized; ectoplacental and exocoelomic cavities had not formed (Fig. 6D, lower panels). In contrast, normal primitive streak stage embryos exhibited well organized ectoderm, endoderm, and mesoderm and developed the ectoplacental, exocoelomic, and amniotic cavities (Fig. 6C, upper panels). The transversal sections demonstrated that the embryonic mesodermal layer was formed between the ectodermal and endodermal layer on the primitive streak side in control embryos (Fig. 6D, upper panels).

DISCUSSION

The present study demonstrates that ARFRP1 is essential for embryonic development. Our data indicate that *Arfrp1*$^{-/-}$ blastocysts are generated and that *Arfrp1*$^{-/-}$ embryos undergo uterine implantation, induce uterine decidualization, and develop into egg cylinders. The embryonic lethality of the *Arfrp1*$^{-/-}$ mutants was specifically associated with the inability of the egg cylinder to gastrulate properly at E6.5 (Fig. 6). At this early stage of gastrulation, morphogenetic movements, cell proliferation, and differentiation convert the embryonic portion of the egg cylinder, the epiblast, into the three germ layers: ectoderm, mesoderm, and endoderm. Epiblast cells are recruited to a transient embryonic structure called the primitive streak at the future posterior pole of the embryo, thereby establishing the anterior-posterior axis (1, 30). At the primitive streak, epiblast cells undergo an epithelial-to-mesenchymal transition, generating the mesoderm and definitive endoderm; *Arfrp1*$^{-/-}$ embryos are defective in this process. The epithelial

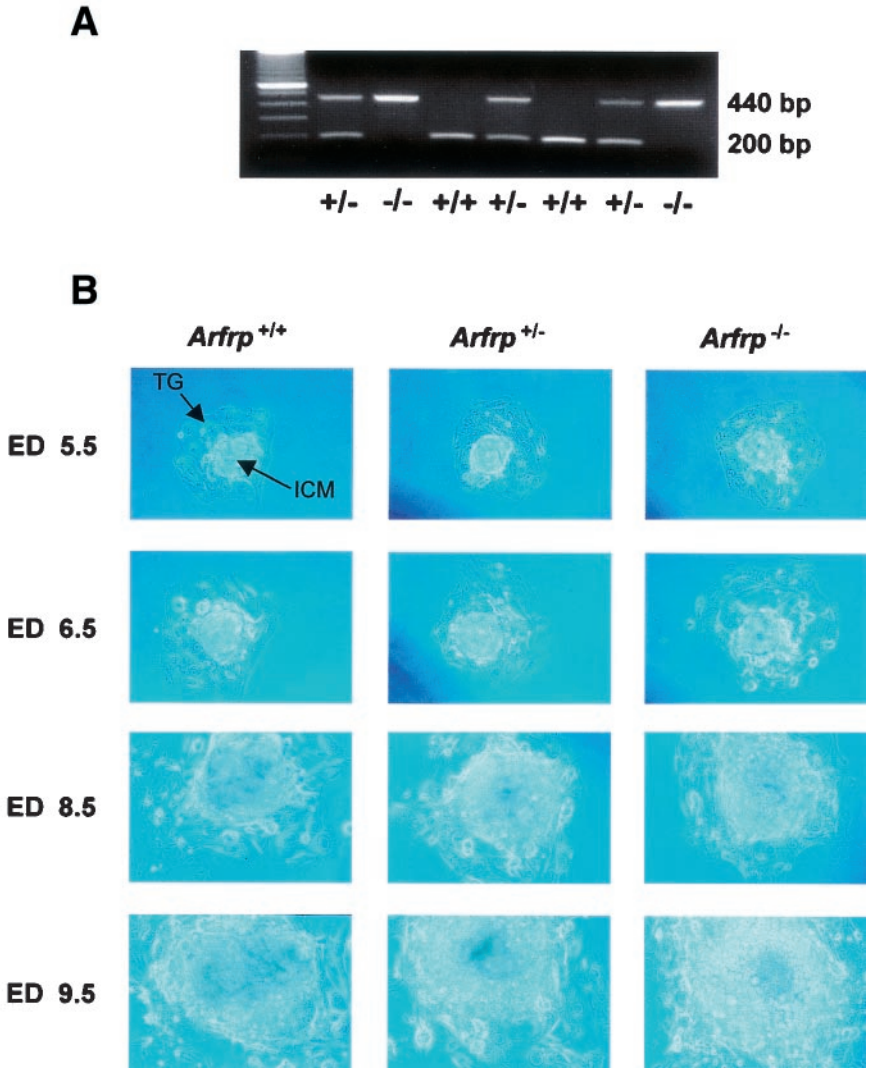

FIG. 4. Growth of *Arfrp1*$^{+/+}$, *Arfrp1*$^{+/-}$, and *Arfrp1*$^{-/-}$ blastocysts in culture. Blastocysts were isolated, cultured, and genotyped as described in Materials and Methods. (A) Genotyping of blastocysts after 8 days of culture with PCR. PCR was performed on genomic DNA of blastocysts with a combination of three primers (two forward primers [1 and 2] and one reverse primer [3]). Primer 1 recognizes sequences in the third intron of *Arfrp1* and is specific to the wild-type *Arfrp1* allele. Primer 2 recognizes sequences of the *neo* resistance gene and is thus mutant allele specific. Primer 3 corresponds to sequences in exon 4. The PCR product of the wild-type allele was 200 bp, and the product of the mutant allele was 440 bp. (B) Outgrowth of *Arfrp1*$^{+/+}$, *Arfrp1*$^{+/-}$, and *Arfrp1*$^{-/-}$ blastocysts after the indicated days in culture. TG, trophoblast giant cells; ICM, inner cellular mass.

organization of the epiblast is disturbed and no mesodermal cells form. Instead, apoptotic cells accumulate in the proamniotic cavity. At this point we cannot determine whether these cells consist of mesendodermal cells which leave the primitive streak in the wrong direction, i.e., towards the dorsal side of the embryo, or whether they represent dying epiblast cells prior to the epithelial-mesenchymal transition.

The targeted inactivation of two other genes, *Rac-1* and β-*catenin*, produced very similar phenotypes. *Rac-1*-deficient embryos exhibit apoptotic cells in the space between the embryonic ectoderm and endoderm at the primitive streak stage (28). Rac-1 is a member of the Rho family of GTPases which has been shown to promote the reorganization of filamentous actin into lamellipodia and membrane ruffles and to be involved in the establishment of cell adhesion structures (13). Moreover, Rac-1 has been implicated in the invasion and metastasis of lymphoma cells (17, 23).

Like *Arfrp1*$^{-/-}$ embryos, β-*catenin* knockout embryos showed cells that detached from the embryonic ectodermal cell layer at E7.0 p.c. (11). β-Catenin is known to regulate cell-cell adhesion via interaction with the cytoplasmic domain of E-cadherin and α-catenin (27). In addition, β-catenin functions as a component in the Wnt signaling pathway, which is involved in the regulation of development, cellular proliferation, and differentiation (18).

The similar phenotypes of *Rac-1*$^{-/-}$, β-*catenin*$^{-/-}$, and *Arfrp1*$^{-/-}$ embryos suggests that ARFRP1 might be involved in the alteration of the cytoskeleton required during gastrulation. Our previous data showing that ARFRP1 inhibits the ARF-regulated PLD activation appears consistent with this hypoth-

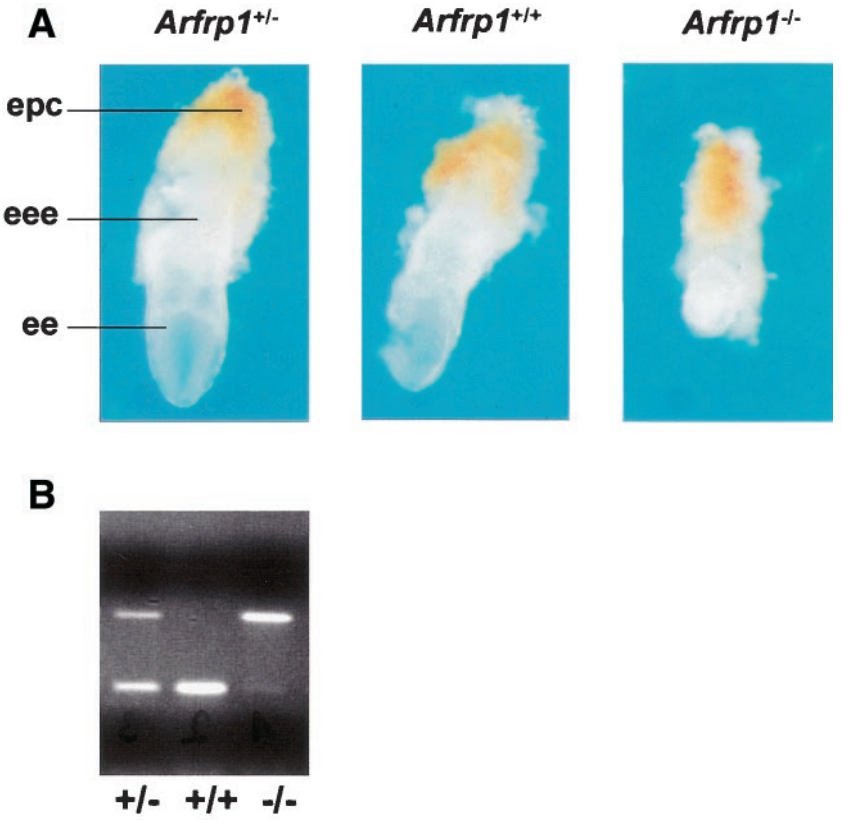

FIG. 5. Comparison of *Arfrp1*$^{+/+}$, *Arfrp1*$^{+/-}$, and *Arfrp1*$^{-/-}$ embryos. Morphological analysis of *Arfrp1* mutant embryos. Whole-mount preparation at E7.5. We analyzed 11 embryos at E7.5 and identified *Arfrp1*$^{+/+}$, *Arfrp1*$^{+/-}$, and *Arfrp1*$^{-/-}$ mutants at a ratio of 1:7:3. epc, ectoplacental cone; eee, extraembryonic ectoderm; ee, embryonic ectoderm.

esis (26). PLD hydrolyzes phosphatidyl choline to generate phosphatidic acid and choline in response to a variety of signals, hormones, neurotransmitters, and growth factors (7, 8). It has been found that agonist-induced PLD stimulation can provoke changes in cell morphology through cytoskeletal rearrangements. Lysophosphatidic acid (LPA)-induced PLD activation has been shown to increase the amount of F-actin leading to an activation of actin polymerization (10). In porcine aortic endothelial cells, PLD activation results in the formation of stress fibers (6). The reduction of endogenous PLD activity by expression of an inactive PLD mutant caused a selective loss of the stress fiber response of LPA (16). In addition, it has been shown that the cytoskeletal protein β-actin inhibits PLD activity by direct binding, suggesting that the agonist-induced translocation of ARF to the membrane might activate the repressed activity of PLD by the actin cytoskeleton (22). Since ARFRP1 inhibits the ARF-stimulated PLD activation (26), one might speculate that a lack of ARFRP1 as a negative regulator of PLD results in alterations of the cytoskeleton.

TABLE 1. Histological analysis of embryos from *Arfrp1*$^{+/-}$ intercrosses[a]

Stage	No. of specimens with phenotype:	
	Normal	Abnormal
E5.5	11	0
E6.5	10	3
E7.5	9	5
E8.5	8	1

[a] Uteri from pregnant *Arfrp1*$^{+/-}$ females that had been mated with *Arfrp1*$^{+/-}$ males were fixed and embedded in paraffin. Serial sections were stained with hematoxylin and eosin or were used for detection of apoptotic cells by TUNEL staining. Embryos were considered abnormal when clusters of TUNEL-positive cells were found within the proamniotic or amniotic cavity (see Fig. 6).

Cell migration is an essential process in embryonic development and is thought to be integrin dependent (2). There is indirect, circumstantial evidence that ARFRP1 might be involved in the regulation of integrin-mediated cell matrix adhesion. Overexpression of cytohesin-1, a protein that interacts with ARFRP1 in a GTP-dependent manner (26), increases β2-integrin-dependent binding of Jurkat cells to ICAM-1 (19). Thus, it is conceivable that the deletion of the *Arfrp1* gene results in defects of integrin-mediated cell adhesion and that this defect results in the failure of dividing epiblast cells to integrate properly into the ectodermal cell layer.

In summary, we present evidence that targeted inactivation of *Arfrp1* results in defective gastrulation, enhanced cell death within the embryonic ectoderm, and a defect in mesendoderm development. We speculate that ARFRP1 plays a critical role in cytoskeletal reorganization or adhesion-dependent morphogenetic processes.

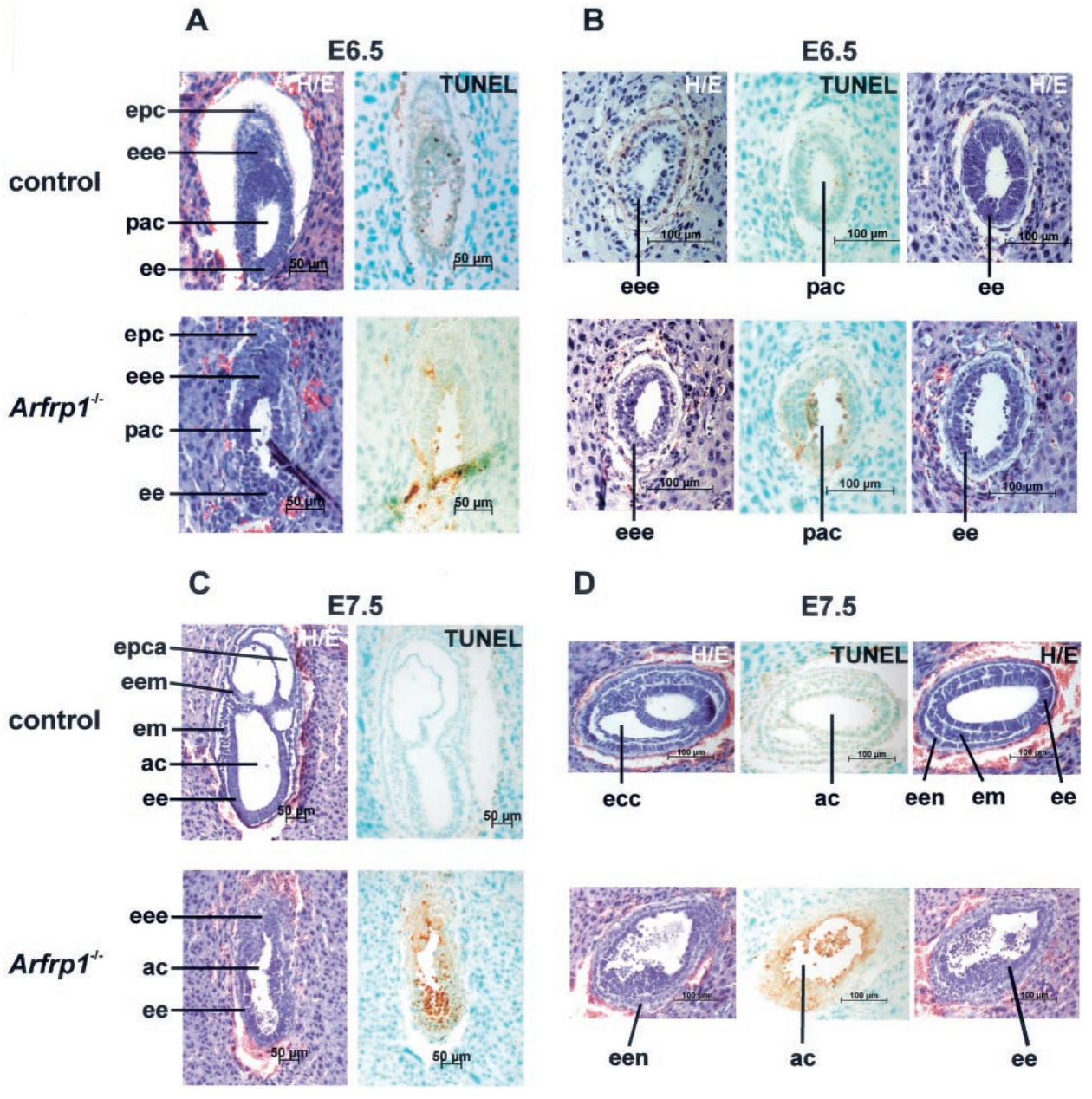

FIG. 6. Apoptotic cell death in *Arfrp1* mutant embryos during gastrulation. Histological analyses of *Arfrp1* mutant embryos. Serial sagittal (A and C) and transversal (B and D) sections of E6.5 (A and B) and of E7.5 (C and D) were prepared and stained with hematoxylin and eosin (H/E) or used for TUNEL assays as described in Material and Methods. ac, amniotic cavity; ecc, extracoelomic cavity; ee, embryonic ectoderm; eee, extraembryonic ectoderm; eem, extraembryonic mesoderm; een embryonic endoderm; em, embryonic mesoderm; epc, ectoplacental cone; epca, ectoplacental cavity; pac, proamniotic cavity.

ACKNOWLEDGMENTS

This work was supported by the Deutsche Forschungsgemeinschaft (Schu 750/3-3).

We thank H.-G. Frank and A. Heerler for helpful discussions. The skillful technical assistance of Sandra Dahmen and Uta Zahn is gratefully acknowledged.

REFERENCES

1. **Beddington, R. S., and E. J. Robertson.** 1999. Axis development and early asymmetry in mammals. Cell **96:**195–209.
2. **Brakebusch, C., E. Hirsch, A. Potocnik, and R. Fassler.** 1997. Genetic analysis of beta1 integrin function: confirmed, new and revised roles for a crucial family of cell adhesion molecules. J. Cell Sci. **110:**2895–2904.
3. **Cavenagh, M. M., J. A. Whitney, K. Carroll, C. J. Zhang, A. L. Boman, A. G. Rosenwald, I. Mellman, and R. A. Kahn.** 1996. Intracellular distribution of Arf proteins in mammalian cells. Arf6 is uniquely localized to the plasma membrane. J. Biol. Chem. **271:**21767–21774.
4. **Chirgwin, J. M., A. E. Przybyla, R. J. McDonald, and W. J. Rutter.** 1979. Isolation of biologically active ribonucleic acid from sources enriched in ribonuclease. Biochemistry **18:**5294–5299.
5. **Cosson, P., and F. Letourneur.** 1997. Coatomer (COPI)-coated vesicles: role in intracellular transport and protein sorting. Curr. Opin. Cell Biol. **9:**484–487.
6. **Cross, M. J., S. Roberts, A. J. H. Ridley, M. N. Hodgkin, A. Stewart, L. Claesson-Welsh, and M. J. Wakelam.** 1996. Stimulation of actin stress

fiber formation mediated by activation of phospholipase D. Curr. Biol. **6:**588–597.
7. **Exton, J. H.** 1997. Phospholipase D: enzymology, mechanisms of regulation, and function. Physiol. Rev. **77:**303–320.
8. **Exton, J. H.** 1997. New developments in phospholipase D. J. Biol. Chem. **272:**15579–15582.
9. **Garcia-Ranea, J. A., and A. Valencia.** 1998. Distribution and functional diversification of the ras superfamiliy in *Saccharomyces cerevisiae*. FEBS Lett. **434:**219–225.
10. **Ha, K. S., E. J. Yeo, and J. H. Exton.** 1994. Lysophosphatidic acid activation of phosphatidylcholine-hydrolysing phospholipase D and actin polymerization by a pertussis toxin-sensitive mechanism. Biochem. J. **303:**55–59.
11. **Haegel, H., L. Larue, M. Ohsugi, L. Fedorov, K. Herrenknecht, and R. Kemler.** 1995. Lack of β-catenin affects mouse development at gastrulation. Development **121:**3529–3537.
12. **Hakem, R., J. L. de la Pompa, C. Sirard, R. Mo, M. Woo, A. Hakem, A. Wakeham, J. Potter, A. Reimair, F. Biellia, E. Firpo, C. C. Hui, J. Roberts, J. Rossant, and T. W. Mak.** 1996. The tumor suppressor gene Brca1 is required for embryonic cellular proliferation in the mouse. Cell **85:**1009–1023.
13. **Hall, A.** 1998. Rho GTPases and the actin cytoskeleton. Science **279:**509–514.
14. **Huang, C. F., L. M. Buu, W. L. Yu, and F. J. Lee.** 1999. Characterization of a novel ADP-ribosylation factor-like protein (yARL3) in Saccharomyces cerevisiae. J. Biol. Chem. **274:**3819–3827.
15. **Kahn, R. A., T. Terui, and P. A. Randazzo.** 1996. Effects of acid phospholipase D on ARF activities: potential roles in membrane traffic. J. Lipid Mediat. Cell. Signal. **14:**209–214.
16. **Kam, Y., and J. H. Exton.** 2001. Phospholipase D activity is required for actin stress fiber formation in fibroblasts. Mol. Cell. Biol. **21:**4055–4066.
17. **Keely, P. J., J. K. Westwick, I. P. Whitehead, C. J. Der, and L. V. Parise.** 1997. Cdc42 and Rac1 induce integrin-mediated cell motility and invasiveness through PI(3)K. Nature **390:**632–636.
18. **Kikuchi, A.** 2000. Regulation of beta-catenin signaling in the Wnt pathway. Biochem. Biophys. Res. Commun. **268:**243–248.
19. **Kolanus, W., W. Nagel, B. Schiller, L. Zeitlmann, S. Godar, H. Stockinger, and B. Seed.** 1996. Alpha L beta 2 integrin/LFA-1 binding to ICAM-1 induced by cytohesin-1, a cytoplasmic regulatory molecule. Cell **86:**233–242.
20. **Lee, F. J., C. F. Huang, W. L. Yu, L. M. Buu, C. Y. Lin, M. C. Huang, J. Moss, and M. Vaughan.** 1997. Characterization of an ADP-ribosylation factor-like 1 protein in *Saccharomyces cerevisiae*. J. Biol. Chem. **272:**30998–31005.
21. **Lee, F. J., L. A. Stevens, Y. L. Kao, J. Moss, and M. Vaughan.** 1994. Characterization of a glucose-repressible ADP-ribosylation factor (ARF3) from *Saccharomyces cerevisiae*. J. Biol. Chem. **269:**20931–20937.
22. **Lee, S., J. B. Park, J. H. Kim, Y. Kim, J. H. Kim, K.-L. Shin, J. S. Lee, S. H. Ha, P.-G. Luh, and S. H. Ryu.** 2001. Actin directly interacts with phospholipase D, inhibiting its activity. J. Biol. Chem. **276:**28252–28260.
23. **Michiels, F., G. G. Habets, J. C. Stam, R. A. van der Kammen, and J. G. Collard.** 1995. A role for Rac in Tiam1-induced membrane ruffling and invasion. Nature **375:**338–340.
24. **Rothman, J. E.** 1994. Mechanisms of intracellular protein transport. Nature **372:**55–63.
25. **Schürmann, A., S. Massmann, and H.-G. Joost.** 1995. ARP is a plasma membrane-associated Ras-related GTPase with remote similarity to the family of ADP-ribosylation factors. J. Biol. Chem. **270:**30657–30663.
26. **Schürmann, A., M. Schmidt, M. Asmus, S. Bayer, F. Fliegert, S. Koling, S. Massmann, C. Schilf, M. C. Subauste, M. Voss, K. H. Jakobs, and H.-G. Joost.** 1999. The ADP-ribosylation factor (ARF)-related GTPase ARF-related protein binds to the ARF-specific guanine nucleotide exchange factor cytohesin and inhibits the ARF-dependent activation of phospholipase D. J. Biol. Chem. **274:**9744–9751.
27. **Steinberg, M. S., and P. M. McNutt.** 1998. Cadherins and their connections: adhesion junctions have broader functions. Curr. Opin. Cell Biol. **11:**554–560.
28. **Sugihara, K., N. Nakatsuji, K. Nakamura, K. Nakao, R. Hashimoto, H. Otani, H. Sakagami, H. Kondo, S. Nozawa, A. Aiba, and M. Katsuki.** 1998. Rac1 is required for the formation of three germ layers during gastrulation. Oncogene **17:**3427–3433.
29. **Takai, Y., T. Sasaki, and T. Matozaki.** 2001. Small GTP-binding proteins. Physiol. Rev. **81:**153–208.
30. **Tam, P. P. L., and R. R. Behringer.** 1997. Mouse gastrulation: the formation of a mammalian body plan. Mech. Dev. **68:**3–25.